CHARACTERIZATION OF APTAMER FUNCTIONALIZED GOLD ELECTRODES FOR HISTONE DETECTION

Hayley Richardson^{1,2}, Jeffrey Barahona², Gavin Carter², Francis J. Miller Jr.^{3,45}, Edgar Lobaton², and Spyridon Pavlidis^{2*}

¹Department of Materials & Science Engineering, NC State University, USA ²Department of Electrical & Computer Engineering, NC State University, USA ³Department of Medicine, Duke University, USA,

⁴School of Medicine, Wake Forest University, USA, ⁵Salisbury Veterans Affairs Medical Center, USA

ABSTRACT

This paper presents findings on the development of an electrochemical histone sensor using gold electrodes functionalized with a histone-specific RNA aptamer sequence. This has applications for early detection of circulating histones which are associated with increased mortality of critically ill patients. Surface plasmon resonance was used to characterize the electrode functionalization process and examine the specific responses to calf thymus and human histones. Through SPR, we show statistically significant differentiation of the responses between different functionalization processes with p < 0.05 on the active and control flow cells. Electrochemical detection of calf thymus histone is subsequently demonstrated, whereby the importance of the spacer molecule was also studied. Initial sensing results showed a calf thymus histone concentration-dependent sensitivity of 7.8 mV/decade, which is an improvement to similar sensors in this field.

KEYWORDS

Histones, aptamers, electrochemical sensors, surface plasmon resonance, potentiometry.

INTRODUCTION

Extracellular histone proteins are toxic to cells and contribute to the development of acute respiratory dysfunction syndrome (ARDS) and multiple organ dysfunction syndrome (MODS). Serum levels of histones in patients are associated with mortality and can be as high as 3 ng/mL [1]. The early recognition of ARDS/MODS is critical for triaging and treating patients. A rapid, accessible method to detect and monitor elevated histone concentrations could be part of an effective strategy, but no point-of-care sensor for this purpose currently exists.

Affinity electrochemical biosensors rely on the formation of self-assembled monolayers (SAM) to serve as the interface with biological medium under analysis (Fig. 1). SAM creation is a key processing step for affinity sensing since the assembled molecules are crucial biorecognition elements (BREs) used to detect specific analytes or stimuli in an electrolyte. Aptamers are advantageous BREs in sensing because they can have high specificity to densely charge analytes and can be easily chemically modified for different applications [2]. Aptamers have also been employed as therapeutics.

Urak et al. published research on the design of several RNA aptamer sequences that selectively bind to both human and bovine histones [1]. Their work used immobilized histones on gold surface then measured aptamer binding to histones; however, this system was not developed with the intention of making an operable sensor, rather only as a functionalized chip for the purpose of verifying the binding activity in surface plasmon resonance (SPR) characterization. Ultimately, their study demonstrated the efficacy in aptamers as treatment of clinical conditions associated with MODS. The sensor in this paper is the reverse system of the one prepared in Urak's study. Here, the aptamers are the immobilized ligand and histones are the analyte in solution.

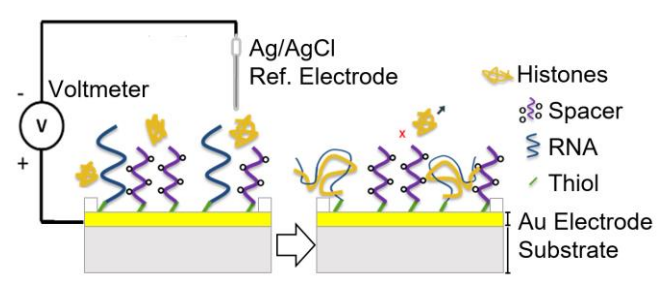


Figure 1: Cross-section of a functionalized gold electrode surface with a thiolated, histone-specific RNA aptamer and a spacer molecule (e.g., MCH or PEG-thiol). An off-electrode Ag/AgCl reference electrode was used.

The objectives of this study are to characterize the behavior of gold electrodes functionalized with histone-specific RNA aptamers, and subsequently assess their suitability for potentiometric detection. Initially, SPR was used to evaluate the ability of immobilized molecules to bind analytes from external solution. Since SPR is a mass-sensitive and optical technique, it is not affected by the ionic composition of the running buffer. Thus, this approach uncouples the measured binding interaction from any ionic non-specific binding that could arise when sensing in typical undiluted buffer solutions or serum [3]. Following observation of the binding kinetics via SPR, potentiometric sensing was evaluated. The important role of 6-mercaptohexanol (MCH) and poly(ethylene glycol) methyl ether thiol (PEG-thiol) molecules in determining non-specific adhesion was determined. These results represent the first report of an electrochemical histone sensor using RNA aptamer recognition elements, and therefore represent a significant step towards the realization of point of care injury monitoring

METHODS

Materials

Analytes calf thymus histone (CTH) and bovine serum albumin (BSA), spacer molecules 6-mercaptohexanol (MCH) and poly(ethylene glycol) methyl ether thiol (PEG-thiol), and regeneration chemicals NaOH and NaCl were all purchased from Sigma Aldrich [St. Louis, MO]. The other analytes of human histones H3.2 and H4 were purchased from New England Biolabs [Ipswich, MA].

The aptamer sequence 5'-Thiol-MC6-S-S-GGG AGG ACG AUG CGG ACU GGU GAA GGG AGG UAC UGC AGA CGA CUC GCC CGA-3' was synthesized by Integrated DNA Technologies (IDT) Inc. [Coralville, IA] and purchased together with TE resuspension buffer (10 mM tris(hydroxymethyl) aminomethane and 0.1 mM ethylenediaminetetraacetic acid). The aptamer was received dried and resuspended according to a previously reported method [4].

SPR consumables of HBS-EP+ running buffer (0.1 M HEPES, 1.5 M NaCl, 0.03 M EDTA and 0.5% v/v Surfactant P20) and sensor chips were purchased from Cytiva [Marlborough, MA].

Surface Plasmon Resonance

As noted above, a thiol modification was added to the 5' sequence end of the aptamer to tether it to gold surfaces. Alkanethiol compounds have been shown to organize on gold and form functional monolayers for a variety of applications [5]. The RNA aptamer was immobilization in-situ on a blank gold sensor chip in a Biacore T200 instrument. 1 μ M aptamer solution was flowed on the active channel for 15 hours at 1 μ L/min. 1 mM MCH was flowed on the active channel and control channel for five hours at 1 μ L/min. Histone dilutions from 1.35 nM to 200 μ M were solubilized in HBS-EP+. Dilutions of BSA were made with the same procedure. Binding was performed with a 180 second association injection and 600 second dissociation phase at 30 μ L/min. Regeneration was done with a solution containing 50 mM NaOH and 1 M NaCl for 60 seconds at 30 μ L/min with a 30 second baseline stabilization before injection the following concentration.

Potentiometric Sensor Electrode Functionalization

The SAM was formed overnight under ambient conditions following the previously reported method [4]. Separately, MCH or PEG-thiol spacer molecules were co-immobilized in the monolayer to aid in the dispersion and support of the aptamer molecules. Spacer molecules help reduce electrostatic charge repulsion and steric hindrance by physically distancing neighboring biorecognition elements [6]. Additionally, they limit potential non-specific adhesion (NSA) of analytes to bare gold surfaces and other biofouling from compounds in the solution.

Potentiometry

Potentiometric tests were done on thin-film gold electrodes from Micrux Technologies [Gijón, Spain] and tested in their benchtop multifluidic platform. The Ag/AgCl reference electrode was purchased from Microelectrodes, INC [Bedford, NH].

Potentiometric sensing tests were performed with a 1-channel Keysight B2901A Series Precision Source/Measure Unit with a custom designed LabVIEW GUI. The potential was measured between the working electrode and reference electrode. Fluid flow was controlled via a programmable syringe pump. HBS-EP+ buffer was flown through the system at 0.5 mL/min, then flow was terminated so that the buffer could sit stagnant on the electrodes for 10 minutes, after which the measured voltage was recorded for approximately 10 minutes. This process was repeated continuously from lowest to highest concentration.

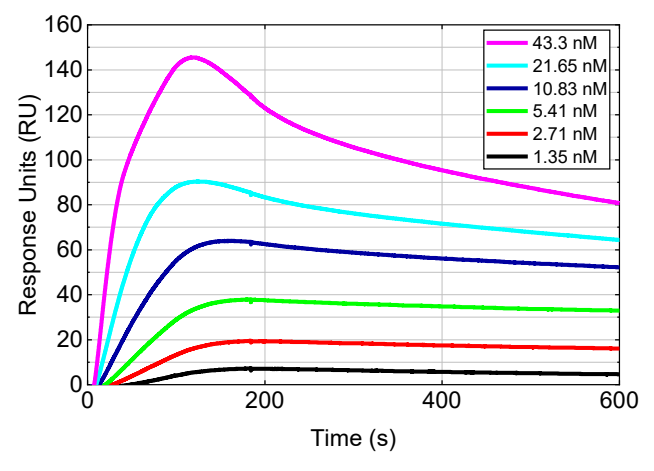


Figure 2: SPR sensogram for CTH from 1.35 to 43.3 nM. This is the aptamer only response, obtained by subtracting the signal produced by the control (MCH-only) surface from the signal produced by the active (aptamer + MCH) surface.

RESULTS & DISCUSSION

Surface Plasmon Resonance

To confirm the specificity of the aptamer surface and provide binding kinetics values, SPR experiments were performed using CTH and human histones, H3.2 and H4, as the target analytes, and BSA as an orthogonal control protein in 10 mM HBS-EP+ running buffer. The specific response of the aptamer-histone interaction was calculated by subtracting the response of the control surface (MCH only) from the active surface (RNA and MCH). Figure 2 displays the clear, concentration-dependent response that was observed.

Furthermore, a preliminary analysis of the morphological and response magnitude characteristics of the SPR data was completed to determine the separability of histone vs. non-histone inputs, which demonstrated distinct responses between the control and active sensor chips, thus illustrating the effectiveness of different ligand immobilization schemes. It was determined that there was baseline wander on the SPR results. As shown in Figure 3, the wander was uniform across the active and control cells, indicating incomplete regeneration of the flow cells. Future efforts will be made to optimize the regeneration conditions [7]. For this study, we removed the baseline wander from the data and zeroed the beginning of each cycle to view only the differences in response magnitude.

We performed two sets of tests to determine the separability of the histones. For both tests, we aggregated measurements from all the concentrations 3.13 nM to 400 nM sampled on the active and control channels. For the first set of tests, we used the maximum amplitude of the waveform at the end of the association phase of the SPR experiment. For the second set of tests, we used the value of the gradients of the SPR outputs at the beginning of the association phase. We hypothesized that the control surface would have different absorption characteristics, and the analytes would adhere at different rates even if they had similar response magnitudes.

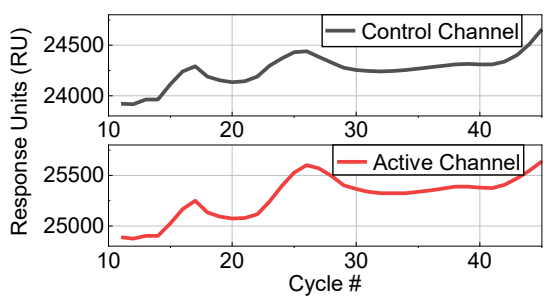


Figure 3: Graphs displaying baseline wander from cycle to cycle. The baseline was determined by the mean of the samples before the association phase begins on any given cycle.

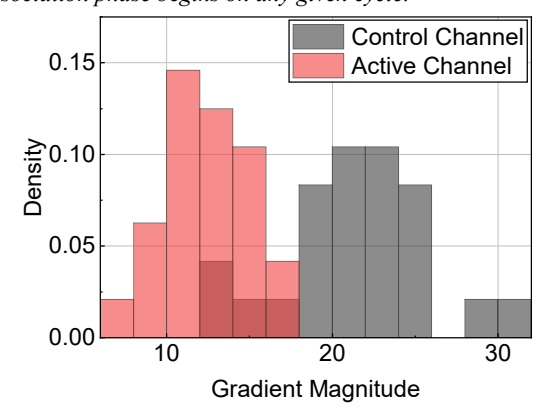


Figure 4: Histograms of the gradient magnitudes at the beginning of the association phase. These demonstrated the distributions of the maximum gradient magnitude of the different channels.

We found that, while the response's amplitude alone does not delineate the difference between control and test surface response to the analytes, the maximum magnitude of the gradients of the SPR outputs allow us to differentiate the active channels from the control channels with p <0.05 (Fig. 4). However, there is insufficient data at the moment to use the same test to differentiate between analytes on the same cell to the same degree of certainty with the same test.

Using a 1:1 binding model, a dissociation constant (K_D) of 0.4 nM was extracted ($\chi^2=9.73~RU^2$). For comparison, SPR experiments originally reported with the characterization of the histone-specific RNA aptamer estimated $K_D=4~nM$ [1]. This discrepancy is attributed to the different surface functionalization methods used in each case and the known heterogeneity of CTH. Figure 5 compares the SPR responses to the various analytes used at a fixed concentration of 200 nM. While H4 induced the highest absolute response in the active channel, the highest differential response was achieved for CTH. The presence of non-specific adhesion (NSA) motivated an investigation of spacer molecules.

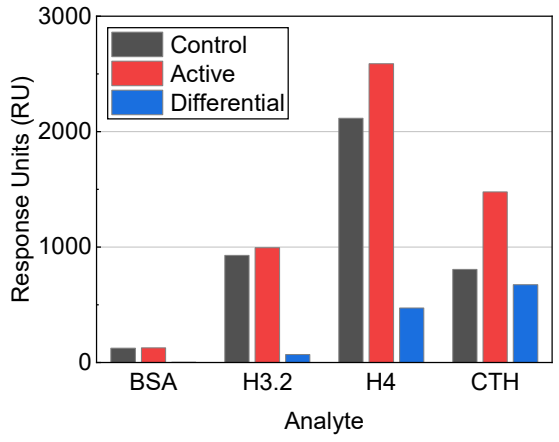


Figure 5: SPR response of the control and active surfaces to 200 nM of CTH, human histones (H3.2 and H4) and BSA. A differential response is also calculated. The active channel exhibits the largest response to H4, and selectivity is highest to CTH.

Potentiometric Sensing

The potentiometric sensor was designed with consideration from the SPR analysis, with output voltage shifts expected due to charge build-up of the bound analyte [8]. These measurements tested concentrations of CTH from 1.56 nM to 1000 nM. The voltage change was measured by subtracting the voltage of an initial buffer baseline from the voltage of the CTH solution after a five-minute stabilization period. Four different types of electrode surfaces were tested: bare gold, MCH, and PEG-thiol controls, and an active surface consisting of aptamer with PEG-thiol.

The appreciable NSA response in the SPR experiments prompted an initial study as to whether MCH could be replaced by PEG-thiol, a different spacer molecule, which may improve the aptamer's performance as a histone-specific BRE. MCH is a short alkanethiol with a six-length carbon chain with a polar hydroxyl head group [-OH]. It is commonly used in nucleotide monolayer formation to remove untethered physiosorbed aptamer from the surface and prevent uptake of unwanted analytes [9] [10]. Its small size ensures that it will backfill the existing space between aptamer to coat any exposed gold and that the aptamers will have sufficient space to fold when bound to histones.

The difference between PEG-thiol and MCH lie in their chain length and the location of their charge polarities in the molecule. The PEG-thiol used in this experiment had a number average

molecular weight of 2 kDa. Instead of the hydroxyl termination like in MCH, PEG-thiol has repeating ether functional groups with electronegative oxygen atoms. This introduces additional charge to the monolayer, but not at the head group [-CH₃] which is most exposed to the histones in solution. Research done by Gutiérrez-Sanz et al. studied PEG blocking with different chain lengths and found that a mix monolayer of receptor antibodies and 10 kDa PEG had three times the signal response compared to a monolayer with antibodies and 0.5 kDa PEG [11].

Comprehensively, there is evidence that longer chain lengths have been found to reduce biofouling and non-specific adsorption, but at the risk of insulating the surface by preventing the charge transfer [12]. Inopportunely, longer chain molecules may prevent proper aptamer tertiary structure upon binding. If the aptamer:histone complex does not fold in close proximity to the electrode surface, the net electrostatic effect of the molecules' binding interaction may be outside of the Debye length (λ_D) [13]. With increasing distance away from the binding interaction, the electric fields generated from the charges are dampened through electrical screening by surrounding charges. The compromise of longer chain length for lower NSA is difficult to predict the results without experimentation since the electrical response will vary depending on the ionic density of the solution and the properties of the analyte [14].

For these reasons, measurements to compare the three different control surfaces were performed before testing the active surface (Fig. 6). While the MCH-coated surface mitigates NSA compared to a bare gold surface, it was found that NSA can be further reduced via the use of PEG-thiol. The differential voltage measurement for the bare gold surface when exposed to 1000 nM CTH was 171.3 mV. MCH and PEG-thiol were only 126.3 mV and 75.1 mV, respectively. If it is assumed that the surface sites between the aptamer are unoccupied if not co-immobilized with another molecule, then the difference between bare gold and PEG-thiol shows a 128% higher NSA voltage response when a spacer molecule is not used. Figure 6 shows the voltage change data for the three control surfaces fit with a logarithmic trendline ($R^2_{Bare\ Au} = 0.98$, $R^{2}_{MCH} = 0.98$, and $R^{2}_{PEG-thiol} = 0.93$). Given that it had the least change in voltage, and thus the least amount of NSA, PEG-thiol was selected as the spacer molecule for subsequent experiments.

An electrode was prepared with histone-specific aptamer and PEG-thiol to compare against the established PEG-thiol control electrode. Figure 7 shows how the change in voltage increased when aptamer was included on the electrode surface. The differential voltage change was calculated the same way as in the control surface comparison data. The co-SAM of aptamer and PEG-thiol data also follow a logarithmic response with $R^2_{\rm Apt,+PEG} = 0.91$.

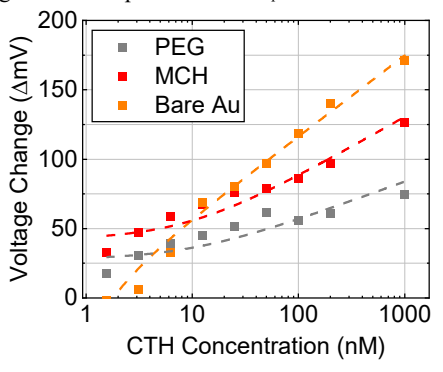


Figure 6: Potentiometric differential voltage response data for control surface of PEG, MCH, and bare gold. The dashed lines are trendlines fitted to the experimental data.

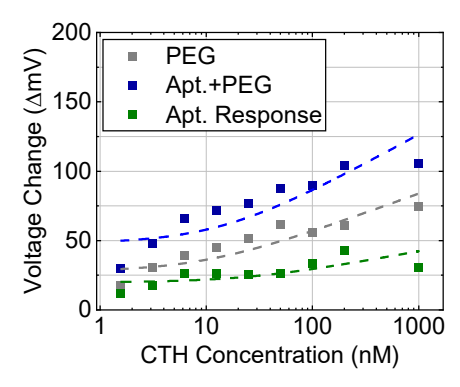


Figure 7: Potentiometric differential voltage response data for the active surface of RNA aptamer and PEG-thiol, the control response of PEG-thiol, and the subtracted voltage change (Apt Response). The dashed lines are trendlines fitted to the experimental data.

As an additional analysis, the voltage response of the PEG-thiol control electrode was subtracted from the aptamer and PEG-thiol active electrode to separate the NSA results from PEG-thiol. This data was plotted as the aptamer response (Fig. 7 "Apt. Response"). The largest calculated aptamer response was 43.2 mV for 200 nM CTH. This sensitivity found in this trendline is 7.8 mV/dec when tested in this type of electrolyte. The ability to test at this low nanomolar concentration was a magnitude improvement when comparing to the published histone sensing done by other groups [15].

CONCLUSIONS

Gold electrode surfaces functionalized with RNA aptamers specific towards CTH and Human Histone H4 have been characterized via SPR, subsequently leading to the first demonstration of potentiometric sensors capable of detecting physiologically relevant concentration of histones. PEG-thiol was the less electrostatically attractive blocking molecule investigated that allowed the aptamer to fold into the correct conformation for specific binding to CTH. This was determined based on the voltage response of different SAMs to different concentrations of CTH. Potentiometric biosensors are ideal low-power systems for the detection of protein molecules because of their sensitivity in physiologically relevant solutions. The isolated response of the CTH-specific aptamers in the monolayer had a sensitivity of 7.8 mV/dec in 10 mM HBS-EP+ when using PEG-thiol as a blocking agent. This sensor was able to detect a discernable signal for the lowest concentration of 1.56 nM CTH.

Further work will electrochemically sense human histones and continue developing classification methods to determine histone vs. non-histone input.

ACKNOWLEDGEMENTS

The authors are grateful for the SPR expertise of Dr. Brian Watts, BIA Core Facility Manager, at the Duke Human Vaccine Institute. This work was made possible by grants from the National Science Foundation (NSF) [Awards ECCS-1936793 (FJM) and ECCS-1936772 (SP and EL)].

REFERENCES

[1] K. T. Urak *et al.*, "RNA inhibitors of nuclear proteins responsible for multiple organ dysfunction syndrome," *Nat. Commun.*, vol. 10, no. 1, p. 116, Jan. 2019, doi: 10.1038/s41467-018-08030-y.

- [2] A. Villalonga, A. M. Pérez-Calabuig, and R. Villalonga, "Electrochemical biosensors based on nucleic acid aptamers," *Anal. Bioanal. Chem.*, vol. 412, no. 1, pp. 55–72, Jan. 2020, doi: 10.1007/s00216-019-02226-x.
- [3] R. L. Rich and D. G. Myszka, "Advances in surface plasmon resonance biosensor analysis," *Curr. Opin. Biotechnol.*, vol. 11, no. 1, pp. 54–61, Feb. 2000, doi: 10.1016/S0958-1669(99)00054-3.
- [4] H. Richardson, G. Maddocks, K. Peterson, M. Daniele, and S. Pavlidis, "Toward Subcutaneous Electrochemical Aptasensors for Neuropeptide Y," in 2021 IEEE Sensors, Oct. 2021, pp. 1–4. doi: 10.1109/SENSORS47087.2021.9639832.
- [5] M. A. Pellitero and N. Arroyo-Currás, "Study of surface modification strategies to create glassy carbon-supported, aptamer-based sensors for continuous molecular monitoring," *Anal. Bioanal. Chem.*, Mar. 2022, doi: 10.1007/s00216-022-04015-5.
- [6] M. Cerruti, S. Fissolo, C. Carraro, C. Ricciardi, A. Majumdar, and R. Maboudian, "Poly(ethylene glycol) Monolayer Formation and Stability on Gold and Silicon Nitride Substrates," *Langmuir*, vol. 24, no. 19, pp. 10646–10653, Oct. 2008, doi: 10.1021/la801357v.
- [7] R. B. M. Schasfoort, "Chapter 1 Introduction to Surface Plasmon Resonance," pp. 1–26, 2017, doi: 10.1039/9781788010283-00001.
- [8] A. Tarasov et al., "A potentiometric biosensor for rapid on-site disease diagnostics," Biosens. Bioelectron., vol. 79, pp. 669– 678, May 2016, doi: 10.1016/j.bios.2015.12.086.
- [9] R. Levicky, T. M. Herne, M. J. Tarlov, and S. K. Satija, "Using Self-Assembly To Control the Structure of DNA Monolayers on Gold: A Neutron Reflectivity Study," *J. Am. Chem. Soc.*, vol. 120, no. 38, pp. 9787–9792, Sep. 1998, doi: 10.1021/ja981897r.
- [10] L. G. Carrascosa, L. Martínez, Y. Huttel, E. Román, and L. M. Lechuga, "Understanding the role of thiol and disulfide self-assembled DNA receptor monolayers for biosensing applications," *Eur. Biophys. J.*, vol. 39, no. 10, pp. 1433–1444, Sep. 2010, doi: 10.1007/s00249-010-0599-6.
- [11] Ó. Gutiérrez-Sanz, N. M. Andoy, M. S. Filipiak, N. Haustein, and A. Tarasov, "Direct, Label-Free, and Rapid Transistor-Based Immunodetection in Whole Serum," ACS Sens., 2017, doi: 10.1021/acssensors.7b00187.
- [12] F. V. Oberhaus, D. Frense, and D. Beckmann, "Immobilization Techniques for Aptamers on Gold Electrodes for the Electrochemical Detection of Proteins: A Review," *Biosensors*, vol. 10, no. 5, May 2020, doi: 10.3390/bios10050045.
- [13] I. M. Bhattacharyya and G. Shalev, "Electrostatically Governed Debye Screening Length at the Solution-Solid Interface for Biosensing Applications," ACS Sens., vol. 5, no. 1, pp. 154–161, Jan. 2020, doi: 10.1021/acssensors.9b01939.
- [14] N. Haustein, Ó. Gutiérrez-Sanz, and A. Tarasov, "Analytical Model To Describe the Effect of Polyethylene Glycol on Ionic Screening of Analyte Charges in Transistor-Based Immunosensing," ACS Sens., vol. 4, no. 4, pp. 874–882, Apr. 2019, doi: 10.1021/acssensors.8b01515.
- [15] T. Goda and Y. Miyahara, "Label-Free Monitoring of Histone Acetylation Using Aptamer-Functionalized Field-Effect Transistor and Quartz Crystal Microbalance Sensors," *Micromachines*, vol. 11, no. 9, Art. no. 9, Sep. 2020, doi: 10.3390/mi11090820.

CONTACT

*S. Pavlidis, tel: +1-919-513-3018; spavlidis@ncsu.edu